# Kinetics of precursor cleavage at the dibasic sites

## Involvement of peptide dynamics

Jean-Marie Glandieres[a], Maud Hertzog[b], Noureddine Lazar[b], Noureddine Brakch[c], Paul Cohen[b], Bernard Alpert[a], Mohamed Rholam[b,*]

[a] *Université Denis Diderot, Laboratoire de Biologie Physico-chimique, 2 Place Jussieu, 75005 Paris, France*
[b] *Université Pierre et Marie Curie, UMR 7631 CNRS, 96 Bd Raspail, 75006 Paris, France*
[c] *Division d'Hypertension, CHU Vaudois, CH-1011 Lausanne, Switzerland*

Received 8 January 2002; revised 20 February 2002; accepted 22 February 2002

First published online 7 March 2002

Edited by Judit Ovádi

**Abstract The presence in the $P'_1$ position relative to the LysArg doublet of either Phe, Tyr or Trp residues affects only pro-OT/Np(7–15) flexibility. This has a measurable effect on the dynamics of the peptide. Since the same modifications have a major influence on the $K_m$ and $V_{max}$ values of the peptide cleavage, these kinetic parameters should depend on the peptide substrate motions. Therefore, the primary kinetic contribution of substrate cleavage should arise from substrate dynamics rather than from the enzyme.** 

*Key words:* Peptide dynamics; Pro-ocytocin/neurophysin peptide substrate; Proteolytic cleavage kinetics; Fluorescence lifetime; Quenching

## 1. Introduction

Proteolytic cleavage of peptide and protein precursors at dibasic amino acids constitutes one of the crucial post-translational events leading to active molecules [1–3]. In these precursors, the processing sites share in their vicinity reverse turns [4] or loops [5], structures providing readily accessible regions for selective proteases [1]. Although these particular structural features constitute recognition signals for the processing enzyme machinery [1,6–10], nothing is known about the mechanism producing the rate value of the cleavage process. This is clearly shown by a series of peptides reproducing, or mimicking, the dibasic cleavage site of the ocytocin/neurophysin precursor (pro-OT/Np) [1]. Indeed, the replacement of $Ala^{13}$ ($P'_1$ position) by various amino acid residues changed both the cleavage rate of the pro-OT/Np(7–15) segment and its affinity for the protease [11].

Topological changes between these peptide substrates or variant plasticity of the dibasic cleavage site could be the underlying factors in the specification of the proteolysis rate [12]. More specifically, internal motions of pro-OT/Np(7–15) peptide analogs could be directly linked to the kinetic process of their cleavage. So, to determine the contributions from the structure and from the dynamics in this kinetic process, pro-OT/Np(7–15) peptides, bearing Phe, Tyr and Trp amino acid residues at the $P'_1$ position [11], were analyzed. Thus, their far-UV circular dichroism (CD) properties were used to monitor their secondary structure variability. Their plasticity and their peptide motions (near the dibasic site) were evaluated by measuring the aromatic residue fluorescence properties (lifetime distribution and quenching kinetics).

## 2. Materials and methods

### 2.1. Peptides

Pro-OT/Np(7–15) analogs (Table 1) were synthesized and purified as described [10].

### 2.2. Optical absorbance and CD measurements

Optical absorbances were obtained on a Varian Cary 3E spectrophotometer. CD spectra were collected on a Jobin Yvon Mark VI dichrograph. Measurements in the far-UV (190–250 nm) were performed in $H_2O$. Results are expressed as mean residue ellipticity $[\theta]_R$ (° $cm^2$ $dmol^{-1}$).

### 2.3. Steady-state fluorescence measurements

Steady-state fluorescence was performed on an Aminco–Bowman spectrofluorometer. Excitation and emission bandwidths were 2 and 4 nm, respectively. Optical densities were less than 0.1 at 265 nm for Phe, 275 nm for Tyr and 295 nm for Trp.

### 2.4. Time-resolved fluorescence measurements

Fluorescence decays were determined by a single-photon counting method using synchrotron radiation (Super-Aco (LURE)) as a source of UV exciting light. The fluorescence was collected at right angle to the incident beam and through a polarizer set at the magic angle (54.7°). Emitted photons were stored in 2048 channels of 25 ps width. Each fluorescence decay curve $\varphi(t)$ contained $5\times10^6$–$10^7$ counts. The apparatus response function $g(t)$ was measured with a scattering solution and alternately with the fluorescence emission.

The measured fluorescence decay has the form: $\varphi(t) = g(t)*\int\alpha(\tau)\, e^{-t/\tau}\, d\tau$, where * denotes the convolution product and $\alpha(\tau)$ the pre-exponential factor distribution of the decay time $\tau$. The curves $\varphi(t)$ were deconvoluted and analyzed using the maximum entropy method [13].

The fluorescence signal of samples was expressed as: $F(t) = \Sigma\alpha_i$

Table 1
Amino acid sequence of the pro-OT/Np(7–15) domain and peptide analogs

| Peptide substrates | | Peptide sequences |
|---|---|---|
| [$Ala^{13}$]pro-OT/Np(7–15): | $A^{13}$ | P-L-G-G-K-R-**A**-V-L |
| [$Trp^{13}$]pro-OT/Np(7–15): | $W^{13}$ | P-L-G-G-K-R-**W**-V-L |
| [$Tyr^{13}$]pro-OT/Np(7–15): | $Y^{13}$ | P-L-G-G-K-R-**Y**-V-L |
| [$Phe^{13}$]pro-OT/Np(7–15): | $F^{13}$ | P-L-G-G-K-R-**F**-V-L |

*Corresponding author. Fax: (33)-1-42 22 13 98.
*E-mail address:* rholam@ccr.jussieu.fr (M. Rholam).

0014-5793/02/$22.00 
PII: S0014-5793(02)02505-X

$e_i^{-t/\tau}$, where $\alpha_i$ is the amplitude probability correlated to the $i$-th rotamer population and $\tau_i$ its fluorescence decay time. The intensity-weighted average lifetime $\tau_0$ was used in quenching experiments [14]: $\tau_0 = \Sigma f_i \tau_i$ where $f_i = \alpha_i \tau_i / \Sigma \alpha_i \tau_i$.

*2.5. Fluorescence quenching experiments*

Fluorescence intensity quenchings were analyzed by using the Stern–Volmer representation [15]: $F_0/F = 1 + K_{sv}[Q]$, where $F_0/F$ is the ratio of the fluorescence intensity in the absence and the presence of the quencher, [Q] is the quencher concentration of dichloroacetamide (DCA) and $K_{sv}$ is the Stern–Volmer quenching constant. In collisional fluorescence quenching: $K_{sv} = k_q \tau_0$, where $k_q$ is the kinetic quenching constant.

## 3. Results

*3.1. Structural characterization of the pro-OT/Np(7–15) peptide models*

It was previously shown that the pro-OT/Np(7–15) peptide analogs are characterized in solution by a conformational equilibrium between aperiodic structures and β-turns [1]. Similar CD spectra were obtained for the $F^{13}$, $Y^{13}$ and $W^{13}$ peptides (Fig. 1), indicating that the native β-turn conformational state was maintained with their permanent interchanges [1].

*3.2. Structural flexibility of each species*

Absorption spectra of the $W^{13}$, $Y^{13}$ and $F^{13}$ peptides resemble the absorption of free Phe, Tyr and Trp in the 250–300 nm region. Their steady-state fluorescence spectra also exhibit the same characteristics as those of the isolated residues dissolved in aqueous buffer [16,17]. The fact that the shapes of absorption and emission spectra are conserved suggests that these residues were in contact with the aqueous solvent without any conformational change of pro-OT/Np(7–15) peptides (see CD data). However, as observed for other peptides [16–18], their fluorescence quantum yields are smaller than that of the free residues. These lower values result mainly from peptide bonds and inductive effects as proton transfer and electron-withdrawing [19–21]. These effects – more or less facilitated by peptide fluctuations – are induced by specific intramolecular interactions which define the particular rotamer distribution of each fluorophore inserted in the original $A^{13}$ peptide. Indeed, each fluorescent amino acid exhibits three rotamers whom the interconversion rates depend on peptide constraints [17,22,23].

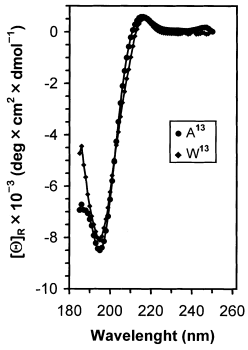


Fig. 1. Far-UV CD spectra of the $F^{13}$, $Y^{13}$ and $W^{13}$ peptides in $H_2O$ (pH 5.5). The experimental CD lines are distributed between the two extrema given profiles. Observed differences are within the precision limit of the apparatus. Measurements were performed at 25°C on 50 μM peptide solutions made in $H_2O$.

When the exchange rates between the rotamers are slower than their fluorescence decay kinetics [17,22,23], each rotamer exhibits its own fluorescence lifetime and the weights of the fluorescence decays represent the rotamer populations. Since the rate of rotamer distribution is determined by the peptide dynamics, a rise in temperature – increasing the peptide motions – may accelerate the interconversion rates and then changes rotamer distribution. We have used the evolution of the fluorescence decay populations with temperature (from 10 to 40°C) to establish the role of Phe, Tyr and Trp residues in the flexibility of the pro-OT/Np(7–15) peptide. A single fluorescence lifetime was found for each of the free amino acids in aqueous buffer pH 7.5 (Table 2), indicating that exchange rates between the three rotamers are faster than their respective fluorescence decay times. In contrast, two or three components were observed in the fluorescent decay of pro-OT/Np(7–15) peptides, depending upon the temperature and the nature of the fluorescent amino acid (Fig. 2, Table 2). In the case of $W^{13}$ peptide, whatever the temperature, the transition between the three rotamers occurred over a longer time than their fluorescence decay time. For the two other peptides, two main components were present at all temperatures. The ex-

Table 2
Fluorescence decay parameters of Trp, Tyr and Phe residues either free in phosphate pH 7.5 buffer or inserted in the pro-OT/Np(7–15) peptide sequence

| $T$ (°C) | Free amino acids | Peptides | | | | | | |
|---|---|---|---|---|---|---|---|---|
| | $\tau_0$ (ns) | $\tau_1$ (ns) | $\alpha_1$ (%) | $\tau_2$ (ns) | $\alpha_2$ (%) | $\tau_3$ (ns) | $\alpha_3$ (%) | $\tau_0$ (ns) |
| | Trp | $W^{13}$ | | | | | | |
| 10 | 4.1 | 0.3 | 18 | 1.4 | 15 | 3.8 | 67 | 4 |
| 20 | 3.3 | 0.3 | 17 | 1.3 | 14 | 2.9 | 69 | 3 |
| 30 | 2.6 | 0.3 | 16 | 1.2 | 13 | 2.45 | 71 | 2.3 |
| 40 | 1.8 | 0.3 | 15 | 1.1 | 12 | 2.0 | 73 | 1.85 |
| | Tyr | $Y^{13}$ | | | | | | |
| 10 | 3.3 | 0.9 | 25 | 2.4 | 73.5 | 4.3 | 1.5 | 2.3 |
| 20 | 3.1 | 0.7 | 25 | 2 | 74 | 4.3 | 1.0 | 1.9 |
| 30 | 2.8 | 0.45 | 24 | 1.6 | 76 | | | 1.5 |
| 40 | 2.6 | 0.35 | 24 | 1.5 | 76 | | | 1.4 |
| | Phe | $F^{13}$ | | | | | | |
| 10 | 8 | 0.6 | 14 | 4.5 | 7 | 10 | 79 | 9.7 |
| 20 | 7.3 | | | 4.2 | 11 | 7.5 | 89 | 7.3 |
| 30 | 6.8 | | | 3.5 | 14 | 5.6 | 86 | 5.6 |
| 40 | 6.2 | | | 3.1 | 18 | 4.6 | 82 | 4.4 |

The rotamer population ($\alpha_i$) and their corresponding fluorescence decay ($\tau_i$) were obtained from Fig. 2.

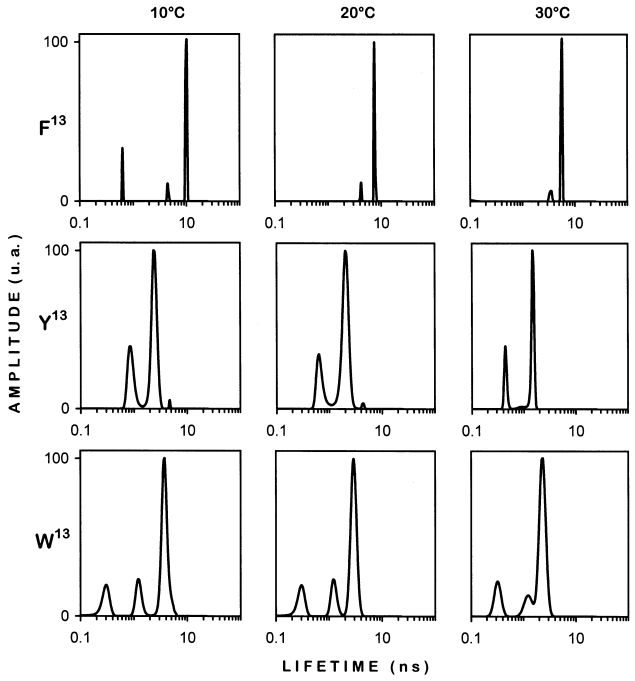


Fig. 2. Fluorescence decay time distribution of Trp, Tyr and Phe residues inserted in the pro-OT/Np(7–15) peptide sequence, as a function of temperature. The pattern gives the pre-exponential factor $\alpha$ versus the fluorescence decay time $t$ values on a logarithm scale. The lifetime behavior is unchanged between 30 and 40°C. Time resolution: 25 ps/channel. Counts: $10^7$ photons.

change time of the third rotamer was found to be longer than its fluorescence decay time only at given temperatures, i.e. $\leq$10°C for $F^{13}$ and $\leq$20°C for $Y^{13}$ peptide substrates. The changes in the relative amplitude of fluorescence decays with the temperature reveal that peptide internal motions (depending upon their elasticity) are modulated by the nature of the $P'_1$ residue: the lower the fluorescence decay number is, the higher is the peptide flexibility. Therefore, peptide flexibility, depending on the nature of the residue inserted at the $P'_1$ position, decreases in the following order: $F^{13} > Y^{13} > W^{13}$.

### 3.2. Peptide-averaged motions

To estimate quantitatively the internal motions of these peptides, their respective fluorescence quenching was assayed in the presence of the same collisional quencher [14]. As shown in Fig. 3, the fluorescence of $F^{13}$, $Y^{13}$ and $W^{13}$ peptides was indeed inhibited by DCA, a quencher with an efficiency equal to the unit [15]. Fig. 4 displays an example of the Stern–Volmer representation [24] of the quenching data at a given temperature. The values of the kinetic quenching constant $k_q$ were determined for the pro-OT/Np(7–15) peptides and the isolated fluorophores (Table 3) from the slopes $K_{sv}$ of their respective Stern–Volmer plots at different temperatures. For the free residues, the encounter rate constant $k_q$ reflects the velocity of the DCA displacement in their neighboring aqueous space [15,25]. In this case, $k_q$ is a function of the viscosity ($\eta$) and of the temperature ($T$) of the solvent: $k_q = c^{te} \times T/\eta$ (Fig. 5). Unexpectedly, quenching of $F^{13}$, $Y^{13}$ and $W^{13}$ peptides exhibits also the same linear dependence (Fig. 5), indicating that the fluorescence collisional quenching of peptide residues is essentially due to migration of DCA quencher molecules within the water medium in their close vicinity [15,24–26]. Such an interpretation is consistent with the fact that the slopes of the straight lines obtained for each peptide were smaller than that found for the free amino acids (see values in parentheses in Fig. 5). The latter observation demonstrates that the parameter $k_q$ is not solely related to the medium viscosity, but reflects also peptide elasticity factors. In order to evaluate the contribution of pro-OT/Np(7–15) peptide internal self-friction to the collisional process [14], the slopes of straight lines $k_q = f(T/\eta)$ obtained for each residue either free or inserted in the peptide (Fig. 5) were compared. The ratio values of these slopes show that free Phe, Tyr and Trp are quenched 3.1, 7.5 and 15% faster than the buried residues in peptides $F^{13}$, $Y^{13}$ and $W^{13}$, respectively. Therefore, this ratio is a good indicator of peptide dynamics.

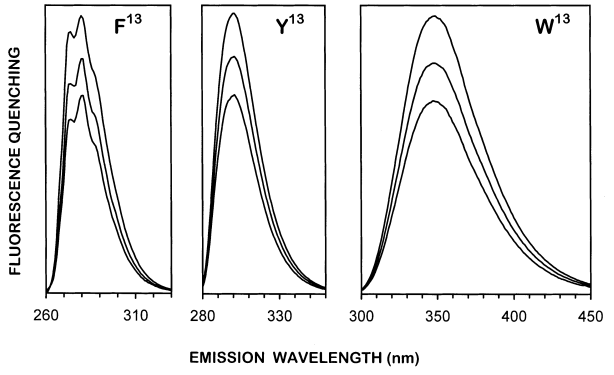


Fig. 3. Inhibition by the same collisional quencher (DCA) of Phe, Tyr and Trp residues inserted in the $A^{13}$ peptide. The figure shows the progressive decrease of the fluorescence spectra when the DCA concentration increased from 0 to 25 mM for $F^{13}$, 0 to 55 mM for $Y^{13}$ and 0 to 28 mM for $W^{13}$.

## 4. Discussion

These data reveal that pro-OTNp(7–15) peptide analogs are characterized, in aqueous solution at pH 7.5, by structural fluctuations depending upon the substituted residue for $Ala^{13}$. The collisional rate constant between DCA inhibitor and the $F^{13}$ peptide has almost the same magnitude as that measured for the isolated Phe in aqueous solution. This provides evidence that this residue, inserted in the peptide, is accessible via the fast internal motions of the $F^{13}$ peptide. As $Phe^{13}$, $Tyr^{13}$ and $Trp^{13}$ are similarly exposed in peptide structure, but their fluctuations are reduced with respect to the $A^{13}$ peptide.

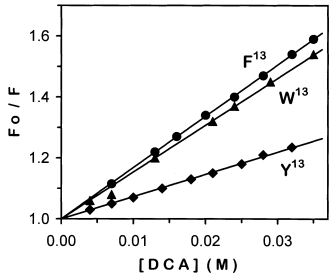


Fig. 4. Stern–Volmer plots of $F^{13}$, $Y^{13}$ and $W^{13}$ fluorescence quenching by DCA at 20°C. $F_0$ and $F$ are the fluorescence intensities of each residue in the absence and in the presence of DCA, respectively.

Table 3
DCA collisional constants on Trp, Tyr and Phe either inserted in the pro-OT/Np(7–15) peptide or as free residues in solution

| $T$ (°C) | Free amino acids $K_{sv}$ ($M^{-1}$) | $k_q = K_{sv}/\tau_0$ ($10^9$ $s^{-1}$ $M^{-1}$) | Peptides $K_{sv}$ ($M^{-1}$) | $k_q = K_{sv}/\tau_0$ ($10^9$ $s^{-1}$ $M^{-1}$) |
|---|---|---|---|---|
| | Trp | | $W^{13}$ | |
| 10 | 18.4 | 4.5 | 15.5 | 3.9 |
| 20 | 19.4 | 5.9 | 15.5 | 5.15 |
| 30 | 20.0 | 7.7 | 15.5 | 6.7 |
| 40 | 17.3 | 9.6 | 15.5 | 8.4 |
| | Tyr | | $Y^{13}$ | |
| 10 | 10.4 | 3.1 | 6.6 | 2.9 |
| 20 | 13.0 | 4.2 | 7.35 | 3.9 |
| 30 | 15.4 | 5.5 | 7.6 | 5.1 |
| 40 | 17.9 | 6.9 | 9.0 | 6.4 |
| | Phe | | $F^{13}$ | |
| 10 | 14.0 | 1.75 | 16.8 | 1.7 |
| 20 | 17.5 | 2.4 | 16.8 | 2.3 |
| 30 | 21.0 | 3.1 | 16.8 | 3.0 |
| 40 | 24.1 | 3.9 | 16.8 | 3.8 |

The $K_{sv}$ values are the slopes of the Stern–Volmer representation. The $\tau_0$ values are taken from Table 2.

Our experiments suggest that the peptide flexibility determines the elementary exposure to the solvent of buried residues. For small peptides as the pro-OT/Np(7–15) peptides, internal fluctuations would contribute to make a particular domain accessible for specific chemical reactions. Since these peptides are cleaved with different efficacies [11], our data indicate clearly that these peptide substrates have sufficient mobility to modulate the exposure time of the peptide moieties recognized by the enzyme. Therefore, fluctuations of the processing domain should be connected to proteolytic cleavage of the $A^{13}$ peptide. Indeed, substitution of Trp for Ala decreases both the $K_m$ and the $V_{max}$ of the catalysis by the convertase whereas replacement of Ala by Phe or Tyr increases these values [11]. In other words, since the affinity can be considered as reflected by $1/K_m$, the lesser the affinity of the convertase for its substrates is, the faster appears the rate of peptide hydrolysis. Taken together, the fluorescence and kinetic data suggest that whereas a very flexible pro-OT/Np(7–15) peptide defavors enzyme–peptide complex formation (low $1/K_m$) it enhances the catalysis rate (high $V_{max}$).

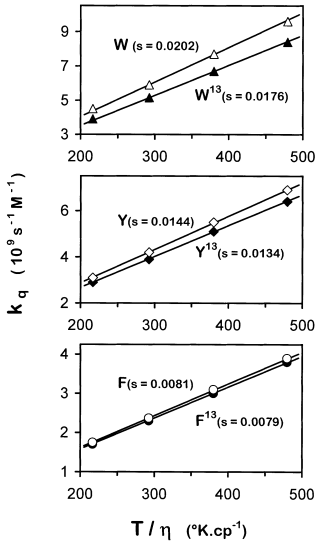


Fig. 5. $T/\eta$ dependence on the rate constant $k_q$ for collisional quenching of $F^{13}$, $Y^{13}$ and $W^{13}$. The values in parentheses give the experimental slope for each plot.

In turn, a peptide of low flexibility will help recognition by the enzyme although it reduces the rate of the catalytic reaction. Therefore, the internal motions of $W^{13}$, $Y^{13}$ and $F^{13}$ substrates have opposite effects on the catalytic parameters of the $A^{13}$ peptide. Such an observation provides a physical basis for a sound interpretation of proteolysis rate values obtained for other pro-OTNp(7–15) substrates in which the $P'_1$ residue was modified [11].

In previous studies [6–9,11], it was shown that dibasic site recognition by processing endoproteases is not correlated with the existence of a consensus primary sequence but rather with the presence of β-turns [4] or large loops [5] around these proteolytic loci. In view of the general role played by this type of secondary structures in a number of biological processes [27,28], it was concluded that the proteases specific for dibasic sites share a common mechanism which allows them to cleave a large variety of distinct precursors or peptide substrates mimicking different prohormone cleavage sites [5–11]. Interestingly, previous crystallographic data have shown that substrate can influence the geometry of the enzyme active site [29]. Variations of the peptide structure are, therefore, one of the critical factors in the proteolytic susceptibility of the enzyme. The present report reveals that internal flexibility of peptide substrates dictates the kinetics of their hydrolysis, providing a rationale for the understanding of the existence of a rather limited number of precursor processing endoproteases [1–3]. In conclusion, our results provide a working model in which proteolytic cleavage at dibasic sites is depending upon peptide substrate dynamics which could be channeled and differently regulated by the associated proteases.

*Acknowledgements:* We thank Dr. F. Merola for his help with fluorescence lifetime measurements and the staff at LURE (Orsay-France) for technical assistance at the synchrotron.

## References

[1] Rholam, M. and Cohen, P. (1997) Anal. Chim. Acta 352, 155–178.
[2] Seidah, N., Mbikay, M., Marcinkiewicz, M. and Chrétien, M. (1998) in: Proteolytic and Cellular Mechanisms in Prohormone Processing (Hook, V., Ed.), pp. 49–76, RG Landes, Georgetown.
[3] Zhou, A., Webb, G., Zhu, X. and Steiner, D. (1999) J. Biol. Chem. 274, 20745–20748.

[4] Rholam, M., Nicolas, P. and Cohen, P. (1986) FEBS Lett. 207, 1–6.
[5] Bek, E. and Berry, R. (1990) Biochemistry 29, 178–183.
[6] Weiss, M., Frank, B., Khait, I., Pekar, A., Heiney, R., Shoelson, S. and Neuringer, L. (1990) Biochemistry 29, 8389–8401.
[7] Rayne, R. and O'Shea, M. (1993) Eur. J. Biochem. 217, 905–911.
[8] Brakch, N., Rholam, M., Boussetta, H. and Cohen, P. (1993) Biochemistry 32, 4925–4930.
[9] Brakch, N., Boileau, G., Simonetti, M., Nault, C., Joseph-Bravo, P., Rholam, M. and Cohen, P. (1993) Eur. J. Biochem. 216, 39–47.
[10] Brakch, N., Rholam, M., Simonetti, M. and Cohen, P. (2000) Eur. J. Biochem. 267, 1626–1632.
[11] Rholam, M., Brakch, N., Germain, D., Thomas, D., Fahy, C., Boussetta, H., Boileau, G. and Cohen, P. (1995) Eur. J. Biochem. 227, 707–714.
[12] Jain, D., Kaur, K. and Salunke, D. (2001) Biophys. J. 80, 2912–2921.
[13] Brochon, J. (1994) Methods Enzymol. 240, 262–311.
[14] Haouz, A., Glandières, J., Zentz, C., Pin, S., Ramstein, J., Tauc, P., Bouchon, J. and Alpert, B. (1998) Biochemistry 37, 3013–3019.
[15] Eftink, M. and Ghiron, C. (1981) Anal. Biochem. 114, 199–227.
[16] Longworth, J. (1971) in: Excited States of Proteins and Nucleic Acids (Steiner, R. and Wecury, B., Eds.), Plenum Press, New York, pp. 319–484.
[17] Ross, J., Wyssbrod, H., Porter, R., Schwartz, G., Michaels, C. and Laws, W. (1992) Biochemistry 31, 1585–1594.
[18] Longworth, J. (1968) Photochem. Photobiol. 8, 589–599.
[19] Seidel, C., Orth, A. and Greulich, K. (1993) Photochem. Photobiol. 58, 178–184.
[20] Chen, Y., Liu, B., Yu, H. and Barkley, M. (1996) J. Am. Chem. Soc. 118, 9271–9278.
[21] Chen, Y. and Barkley, M. (1998) Protein Biochem. 37, 9976–9982.
[22] Szabo, A. and Rayner, D. (1980) Biochem. Biophys. Res. Commun. 94, 909–915.
[23] Ross, J., Laws, W., Buku, A., Sutherland, J. and Wyssbrod, H. (1986) Biochemistry 25, 607–612.
[24] Stern, O. and Volmer, M. (1919) Phys. Z. 20, 183–188.
[25] Lakowicz, J. and Weber, G. (1973) Biochemistry 12, 4171–4179.
[26] Albani, J. and Alpert, B. (1987) Eur. J. Biochem. 162, 175–178.
[27] Laczkò, I., Hollòsi, M., Ürge, L., Ugen, K., Weiner, D., Mantsch, H., Thurin, J. and ÖtvÖs, L. (1992) Biochemistry 31, 4282–4288.
[28] Collawn, J., Stangle, M., Kuhn, L., Esekogwu, V., Jing, S., Trowbride, I. and Tainer, J. (1990) Cell 63, 1061–1072.
[29] Gupta, V., Muyldermans, S., Wyns, L. and Salunke, D. (1999) Proteins 35, 1–12.